Molecular Vibrations of Three Crystal Forms of Poly(vinylidene fluoride)

Masamichi Kobayashi, Kohji Tashiro, and Hiroyuki Tadokoro*

Department of Polymer Science, Faculty of Science, Osaka University, Toyonaka, Osaka, 560 Japan. *Received October 8, 1974*

ABSTRACT: Infrared and Raman spectra in the region from 4000 to 30 cm^{-1} of three crystal forms, namely, I, II, and III, of poly(vinylidene fluoride) $(-CF_2CH_2-)_n$ have been measured. The optically active librational lattice vibration appears at 70, 53, and 84 cm^{-1} in the far-infrared spectra of forms I, II, and III, respectively. The normal frequencies have been calculated for the crystal lattices with the space groups $Cm2m$ (for form I), $P2_1/c$ (form II), and $C121$ (form III), by assuming valence force field intramolecular forces along with van der Waals and electrostatic intermolecular forces. The calculated frequencies of the lattice modes as well as the molecular modes are in good agreement with the observed data. The difference in vibrational spectrum between crystal forms I and III, both consisting of the essentially planar zigzag chains, was interpreted reasonably by the difference in relative height of the chains in the unit cell, as proposed by the previous X-ray work, and, therefore, form III was confirmed as the third crystal phase different from form I. In the spectra of forms I and III there appear many weak bands and band splittings on cooling to liquid nitrogen temperature, which are not associated with the optically active fundamentals of the regular crystal lattices of these forms. Most of them correspond well to the positions of the peaks in the frequency distribution functions computed for forms I and III, and are ascribed to the statistically disordered crystal structures consisting of slightly deflected chains. Some of the weak bands were assigned to the head-to-head linkages incorporated in the sample on the basis of the vibrational analysis made on the alternating copolymer of ethylene and tetrafluoroethylene, a typical model compound of the head-to-head structure. Infrared and Raman spectra of form II, throughout the whole frequency range, have been found to be consistent with the space group $P2_1/c$ proposed by the previous X-ray work.

In a previous paper[1] the authors reported that poly(vinylidene fluoride) (PVDF) crystallizes into three crystal forms, namely, I, II, and III, depending upon the crystallization conditions. The crystal structures of the three forms have been determined in this laboratory by means of X-ray analysis,[2] the crystallographic data being reproduced in Table I. In forms I and III the molecule assumes an essentially planar zigzag conformation, and in form II it has a TGTḠ conformation.

The crystal lattice of form I determined by the authors, somewhat different from the regular orthorhombic lattice proposed by Lando, *et al.*,[3] includes a statistically disordered packing of slightly deflected molecular chains.

As for form III which has been first found as the third crystal phase by Natta, *et al.*,[4] Cortili and Zerbi[5] suggested from the infrared spectroscopic data that this phase consisted of disordered planar zigzag chains. The crystal phase has been referred to phase I′ by Doll and Lando.[6] This phase was regarded by the present authors[1,2] as a new crystal modification with a monoclinic unit cell consisting of essentially planar zigzag chains with slight statistical deflection. The X-ray analysis of form III, however, has been performed by using diffraction data from a powder photograph, since form III was not obtained in a highly oriented form because of simultaneous change to form I during the orientation procedure. The proposed crystal structure would, therefore, be less accurate compared with the other two modifications. Moreover, a close similarity in X-ray diffraction pattern as well as in infrared spectrum of forms I and III makes it obscure to decide whether form III should be regarded as the third crystal phase or not.

As for form II, Doll and Lando[7] have proposed two possible unit cell structures with the space groups $P2_1$ and $P1$, both being different from that proposed by the present authors ($P2_1/c$). The discrepancy was thought, according to Farmer, *et al.*,[8] to be attributed to the difference in the amount of head-to-head linkages involved in the samples used in the two schools.

Thus, there are many problems, which are of much interest but remain unsettled, about packing structure of the PVDF molecules in three crystal modifications. In order to shed light on the problems the crystal structures of PVDF are investigated from the viewpoint of vibrational spectroscopy in the present paper.

Infrared and Raman spectra of PVDF have been studied by Cortili and Zerbi,[5] Enomoto, *et al.*,[9] and Boerio and Koenig.[10] However, the previous workers have been concerned with the molecular modes and the molecular structures but have ignored the intermolecular interactions which are essentially important in order to solve the problems of molecular packings. In the present work the vibrational analyses are made on the three-dimensional crystal lattices of three forms of PVDF taking into account both the intra- and intermolecular forces. On the basis of group theoretical considerations as well as the results of the normal coordinate treatment, the packing structures of the molecules in the crystal lattices are investigated.

Besides the normal frequencies of the optically active factor group modes, the frequency distribution functions including all the normal modes in the first Brillouin zone of forms I and III are calculated. Based on the results, the effects of the defects involved on the vibrational spectra are discussed.

Samples and Spectral Measurements

The samples of PVDF used were of a commercial source, Kynar 201, obtained from Pennwalt Chemical Company. They included the head-to-head linkages of about 10% as estimated by ^{19}F nmr spectrum. The melting point was measured as about 172° with a Perkin-Elmer DSC-1B differential scanning calorimeter and also with a polarizing microscope.

The specimens for spectral measurements, consisting of pure respective crystal form, were prepared as follows.

Form I. Oriented film specimens of form I were obtained either (1) by stretching melt-crystallized specimens (form II) about six times their original lengths at room temperature, or (2) by rolling film specimens cast from dimethylacetamide solution (form III). Unoriented film specimens of form I were found to be prepared by casting films from hexamethylphosphoramide solution at room temperature. Powder samples of form I were obtained by grinding com-

Table I
Crystallographic Data of Three Forms of Poly(vinylidene fluoride)[2]

	Form I	Form II	Form III
Crystal system	Orthorhombic	Monoclinic	Monoclinic
Space group	$Cm2m$-C_{2v}^{14}	$P2_1/c$-C_{2h}^{5}	$C121$-C_2^3
Lattice constants	$a = 8.58$ Å $b = 4.91$ Å c(f.a.)[a] = 2.56 Å	$a = 4.96$ Å $b = 9.64$ Å c(f.a.) = 4.62 Å $\beta = 90°$	$a = 8.66$ Å $b = 4.93$ Å c(f.a.) = 2.58 Å $\beta = 97°$

[a] f.a. = fiber axis.

mercial powder samples (almost form II) for several hours at room temperature.

Form II. Unoriented specimens of form II were prepared either (1) by cooling the melt slowly to room temperature, or (2) by casting films from acetone solution at about 50°. Oriented film specimens of form II were obtained by stretching or rolling unoriented specimens of form II about four times the original lengths at the temperature immediately below the melting point.

Form III. Unoriented specimens of form III were prepared by casting films from dimethylacetamide solution at about 65°. Slow evaporation of the solvent increased the purity of form III.[11] Preparation of oriented specimens of form III is very difficult because this crystal form changes very rapidly to form I by mechanical deformation. A specimen with very slight orientation was obtained by rolling a cast film.

A commercial sample of an alternating copolymer of ethylene and tetrafluoroethylene $[-(CH_2)_2(CF_2)_2-]_n$, Tefzel (Du Pont Chem. Co.), was subjected to investigation as a typical model compound consisting of the head-to-head linkages which are known to be included in the sample of PVDF.[12,13] The copolymer sample used here consists of CH_2CH_2 (47.8 mol %) and CF_2CF_2 (52.2 mol %) measured by elementary analysis, and is highly crystalline giving an X-ray fiber diagram with the fiber period of 5.08 Å (Figure 1).[14] The melting behaviors of this sample measured with a differential scanning calorimeter were essentially the same as those of the copolymer samples having the alternation ratio of 93–97% investigated by Modena, *et al.*[15] Oriented film specimens of the copolymer were prepared by hot rolling at 200°.

The infrared spectra were measured by a Japan Spectroscopic Company DS-402G grating infrared spectrophotometer equipped with an AgCl polarizer (4000–400 cm^{-1}), and by a Hitachi FIS-3 far-infrared spectrophotometer with a wire-grid polarizer (400–30 cm^{-1}).

The Raman spectra were taken by a Japan Spectroscopic Company R750 triple monochrometer Raman spectrophotometer equipped with a photon counter. The 5145-Å line from an argon ion laser was used as the excitation light source. Measurements of the polymeric substances accompanied a great deal of difficulties because of weak Raman intensity compared with strong background due to Rayleigh scattering. In order to distinguish the Raman lines from the natural emissions from the laser light source, the anti-Stokes lines were measured as well as the Stokes lines. Both infrared and Raman measurements were carried out at room temperature as well as at liquid nitrogen temperature.

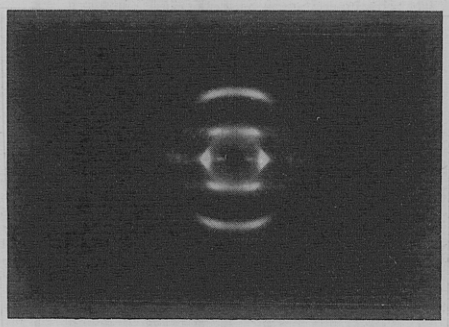

Figure 1. Fiber diagram of the alternating copolymer of ethylene and tetrafluoroethylene.

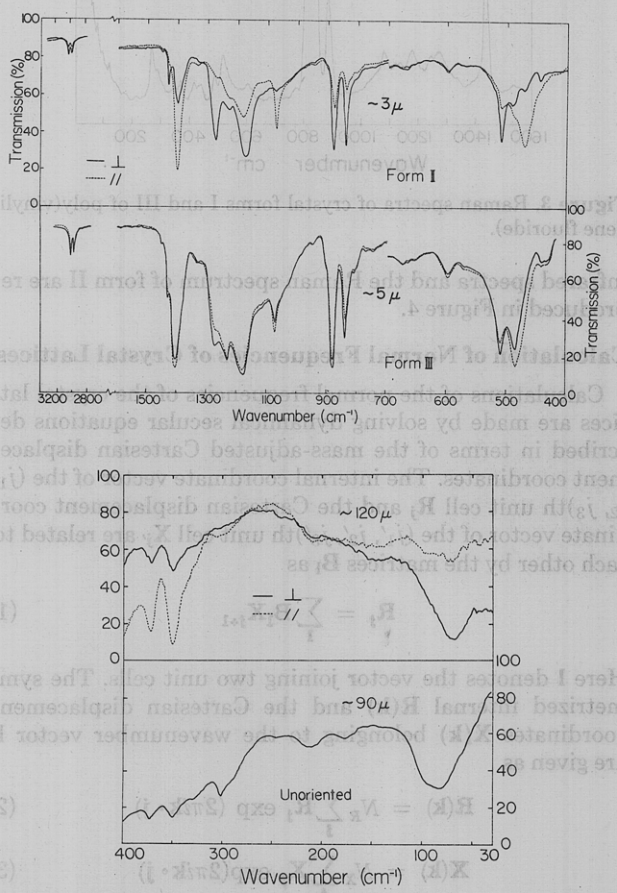

Figure 2. Infrared spectra of crystal forms I and III of poly(vinylidene fluoride) (top) in the region from 4000 to 400 cm^{-1} and (bottom) in the far-infrared region: (——) electric vector ⊥ orientation direction; (- - -) electric vector ∥ orientation direction. The spectrum of form III on the bottom is taken with unpolarized radiation.

The polarized infrared spectra of forms I and III in the region from 4000 to 400 cm^{-1} are reproduced in Figure 2 (top). Here, the solid and broken lines represent the absorptions taken by the infrared radiation with the electric vector perpendicular and parallel to the orientation direction, respectively. A slightly oriented film specimen of form III was used for the measurement. The figures on the absorption curves denote the thickness of the specimens. The far-infrared spectra of forms I and III are compared with each other in Figure 2 (bottom). Here the spectrum of form III was taken with unpolarized radiation, because an oriented film specimen thick enough for the measurement in this region could not be obtained. In Figure 3 are reproduced the Raman spectra of forms I and III. The polarized

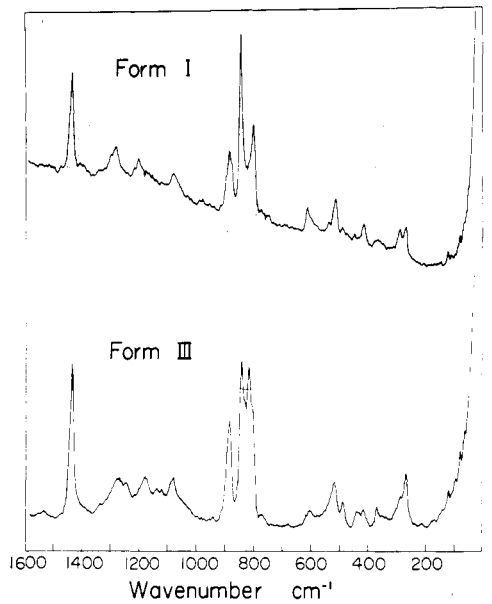

Figure 3. Raman spectra of crystal forms I and III of poly(vinylidene fluoride).

infrared spectra and the Raman spectrum of form II are reproduced in Figure 4.

Calculation of Normal Frequencies of Crystal Lattices

Calculations of the normal frequencies of the crystal lattices are made by solving dynamical secular equations described in terms of the mass-adjusted Cartesian displacement coordinates. The internal coordinate vector of the (j_1, j_2, j_3)th unit cell $\mathbf{R}_j$ and the Cartesian displacement coordinate vector of the (j_1', j_2', j_3')th unit cell $\mathbf{X}_{j'}$ are related to each other by the matrices $\mathbf{B}_l$ as

$$\mathbf{R}_j = \sum_l \mathbf{B}_l \mathbf{X}_{j+l} \tag{1}$$

Here l denotes the vector joining two unit cells. The symmetrized internal $\mathbf{R}(\mathbf{k})$ and the Cartesian displacement coordinates $\mathbf{X}(\mathbf{k})$ belonging to the wavenumber vector $\mathbf{k}$ are given as

$$\mathbf{R}(\mathbf{k}) = N_R \sum_j \mathbf{R}_j \exp(2\pi i \mathbf{k}\cdot\mathbf{j}) \tag{2}$$

$$\mathbf{X}(\mathbf{k}) = N_X \sum_j \mathbf{X}_j \exp(2\pi i \mathbf{k}\cdot\mathbf{j}) \tag{3}$$

and

$$\mathbf{R}(\mathbf{k}) = \mathbf{B}(\mathbf{k})\mathbf{X}(\mathbf{k}) \tag{4}$$

where

$$\mathbf{B}(\mathbf{k}) = \sum_l \mathbf{B}_l \exp(-2\pi i \mathbf{k}\cdot\mathbf{l}) \tag{5}$$

and N_R and N_X are the normalization factors.

The potential energy matrix described in terms of the symmetrized internal coordinates $\mathbf{F}_R(\mathbf{k})$ is given by

$$\mathbf{F}_R(\mathbf{k}) = \sum_l \mathbf{F}_l \exp(-2\pi i \mathbf{k}\cdot\mathbf{l}) \tag{6}$$

where $\mathbf{F}_l$ represents the interactions between two unit cells apart from each other by the vector $\mathbf{l}$. $\mathbf{F}_{000}$ represents the interactions within a unit cell.

The secular equation for the wavenumber vector $\mathbf{k}$ is given as

$$|\mathbf{D}(\mathbf{k}) - \omega^2(\mathbf{k})\mathbf{E}| = 0 \tag{7}$$

$$\mathbf{D}(\mathbf{k}) = \mathbf{M}^{-1/2}\mathbf{B}^{\dagger}(\mathbf{k})\mathbf{F}_R(\mathbf{k})\mathbf{B}(\mathbf{k})\mathbf{M}^{-1/2} \tag{8}$$

Table II
Intramolecular Valence Force Constants of Poly(vinylidene fluoride)

No.	Force constants	Coordinates involved	Common atoms	Values[a] Forms I & III	Form II
1	K_d	CH		4.902	4.902
2	K_R	CC		4.413	4.413
3	F_{Rl}	CC, CF	C	0.403	0.740
4	F_R	CC, CC	C	0.148	0.148
5	$F_{R\gamma}$	CC, CCH	CC	0.206	0.206
6	$F_{R\omega}$	CC, CCC	CC	0.273	0.273
7	$F_{R\phi}$	CC, CCF	CC	0.567	0.567
8	F_d	CH, CH	C	0.058	0.058
9	K_l	CF		5.96	5.96
10	F_{ll}	CF, CF	C	0.621	0.621
11	$F_{l\xi}$	CF, CFF	CF	0.674	0.674
12	H_γ	CCH		0.615	0.615
13	F_γ	CCH, CCH	CC	0.105	0.105
14	F_γ'	CCH, CCH	CH	0.074	0.074
15	H_δ	CHH		0.441	0.481
16	H_ω	CCC		1.248	1.248
17	$f_\omega{}^t$	CCC, CCC(t)	CC	−0.036	−0.036
18	H_ϕ	CCF		1.262	1.262
19	H_ξ	CFF		1.50	1.50
20	T	CCCC		0.05	0.05
21	$F_{l\phi}$	CF, CCF	CF	0.62	0.50
22	F_ϕ	CCF, CCF	CC	0.178	0.178
23	F_ϕ'	CCF, CCF	CF	0.143	0.143
24	$f_\omega{}^g$	CCC, CCC(g)	CC		−0.064
25	$f_{\omega\gamma}{}^g$	CCC, CCH(g)	CC	0.138	0.106
26	$f_{\omega\gamma}{}^t$	CCC, CCH(t)	CC		0.207
27	$f_{\omega\phi}{}^g$	CCC, CCF(g)	CC	−0.085	−0.085
28	$f_{\omega\phi}{}^t$	CCC, CCF(t)	CC		0.239
29	$f_{\gamma\phi}{}^t$	CCH, CCF(t)	CC	0.063	0.063
30	$f_{\gamma\phi}{}^g$	CCH, CCF(g)	CC	0.055	0.055

[a] The stretch constants have units of mdyn/Å; the stretch-bend interactions have units of mdyn/rad; and the bending constants have units of (mdyn Å)/rad².

Here $\mathbf{M}$ is a diagonal matrix consisting of atomic masses and $\mathbf{B}^{\dagger}$ denotes the transposed conjugate complex of $\mathbf{B}$.

The optically active normal modes ($\mathbf{k} = 0$) were calculated for the three crystal forms of PVDF. For forms I and III calculations were also made for the normal modes of the $\mathbf{k}$ vectors within the first Brillouin zone ($k_i = -\frac{1}{2} - \frac{1}{2}$, $i = a, b, c$) of the reciprocal space in order to obtain the frequency distribution functions.

In the present calculations, the intramolecular force constants of valence force field (VFF) type were transferred from those proposed by Boerio and Koenig[10] with slight modification (Table II). Two types of intermolecular force were taken into consideration. One is the van der Waals force acting between nonbonded atoms. The potential energy for an atomic pair at a distance r is given by a Lennard-Jones type potential function

$$V(r) = \epsilon[(r_{min}/r)^{12} - 2(r_{min}/r)^6] \tag{9}$$

where ϵ is the depth of the potential energy minimum, and r_{min} is the position of the minimum potential. The corresponding force constant is given by the second derivative of V with respect to r.

In the present calculations only the H···F atomic pairs were taken into account, since the nonbonded atomic pairs of this kind have interatomic distances shorter than 3 Å in the three crystal lattices. Other kinds of atomic pairs have

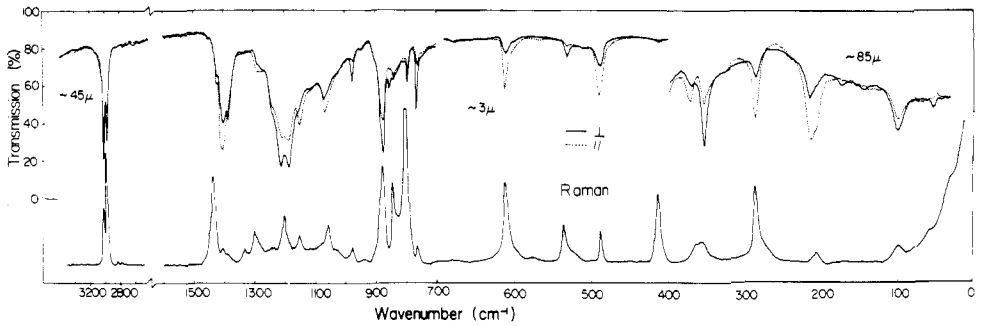

Figure 4. Infrared (upper) and Raman (lower) spectra of crystal form II of poly(vinylidene fluoride). For the infrared absorption: (——) electric vector ⊥ orientation direction; (- - -) electric vector ∥ orientation direction.

Table III
Intermolecular Force Constants of Poly(vinylidene fluoride) Crystals[a]

	Form I		Form II		Form III	
No.	Coordinates involved	Values, mdyn/Å	Coordinates involved	Values, mdyn/Å	Coordinates involved	Values, mdyn/Å
1	ξ_1, ξ_2, ξ_3, ξ_4	0.0163	ξ_1, ξ_5	0.0134	ξ_2, ξ_3	0.0657
2	ξ_5, ξ_6	−0.0021	ξ_2, ξ_7	0.0044	ξ_1, ξ_4	0.0016
3	ξ_7, ξ_8	0.0017	ξ_3	0.0088	ξ_5, ξ_6	−0.0022
4	ξ_9, ξ_{10}, ξ_{11}, ξ_{12}	0.0030	ξ_4, ξ_9	0.0191	ξ_{13}, ξ_{14}	0.0006
5			ξ_6, ξ_8	0.0225	ξ_7, ξ_8	0.0030
6					ξ_9, ξ_{10}, ξ_{11}, ξ_{12}	0.0029

[a] The coordinates involved in the intermolecular force constants are referred to Figure 5.

more distant interatomic distances and give negligibly small contribution to the intermolecular forces. For the parameters of the H···F potential function, the values ϵ = 0.3919 KJ/mol and r_{min} = 2.78 Å were assumed, which have been used in the previous paper[1] for the calculations of the cohesive energies of the crystal lattices of PVDF. The other intermolecular force is due to the electrostatic interaction between the polar groups. Partial charges of 2.104×10^{-10} esu and -1.052×10^{-10} esu were assumed on the carbon and fluorine atoms of the CF_2 groups, respectively, the values being deduced from the CF bond moment of 1.41 D and the CF bond length of 1.34 Å. The Coulombic force constant is given by the equation

$$F(r) = 2Q_1Q_2/Dr^3 \qquad (10)$$

where Q_1 and Q_2 are the amounts of the electric charges on the respective atoms, and D is the dielectric constant which is assumed here to be 4.0. The contribution of the electrostatic interactions is so small (about 10% or less of the total intermolecular interactions) especially in form II that they are taken into account only for the polar crystal lattices of forms I and III. The values of the intermolecular force constants are listed in Table III. The atomic pairs considered in the present calculations are shown schematically in Figure 5.

Vibration of Crystal Form I

The space group of form I has been found as $Cm2m$-C_{2v}^{14} with two chains in the orthorhombic unit cell.[2] Although the X-ray analysis has suggested the statistically disordered packing of slightly deflected chains, the normal modes calculations were made, for the sake of simplicity, for the regular crystal lattice without statistical deflection of the chains. The spectroscopic unit cell contains only one planar zigzag chain in it. The number of the optically active normal modes and the selection rules are obtained as given in Table IV. The calculated normal frequencies are compared with the observed data in Table V. The assignments of the bands are described in terms of potential energy distribution obtained by the calculation for a single molecular chain.

Table IV
Number of the Normal Modes and Selection Rules of Crystal Forms I and III of Poly(vinylidene fluoride)

Species	Molecular modes	Lattice modes	Selection rules: Infrared	Selection rules: Raman
(a) Form I with Space Group $Cm2m$-C_{2v}^{14}				
A_1	5	T_b[a]	Active (⊥)[c]	Active
A_2	2		Forbidden	Active
B_1	3	T_c	Active (∥)	Active
B_2	4	T_a, $L(R_c)$[b]	Active (⊥)	Active
(b) Form III with Space Group $C121$-C_2^3				
A	7	T_b	Active (⊥)	Active
B	7	T_a, T_c, $L(R_c)$	Active (⊥, ∥)	Active

[a] T_a, T_b, T_c: pure translation along the respective crystal axis. [b] $L(R_c)$; librational lattice mode around the fiber axis. [c] ⊥ and ∥ in parentheses denote infrared polarization for a uniaxial specimen.

From Table IV we can expect only one librational lattice mode (B_2 species) in both infrared and Raman spectra. This is clearly assigned to the perpendicular absorption with the peak at 70 cm^{-1}. The calculated normal frequency of the mode is 72 cm^{-1}, in good agreement with the observed one. The librational mode is represented schematically with the $\mathbf{L}_x$ vectors as shown in Figure 6. The calculated frequencies of the intramolecular modes are also in good agreement with the observed infrared and Raman frequencies as given in Table V. The assignments of the intramolecular modes are essentially the same as those given by previous workers.[5,9,10]

Thus, the main infrared and Raman bands are interpret-

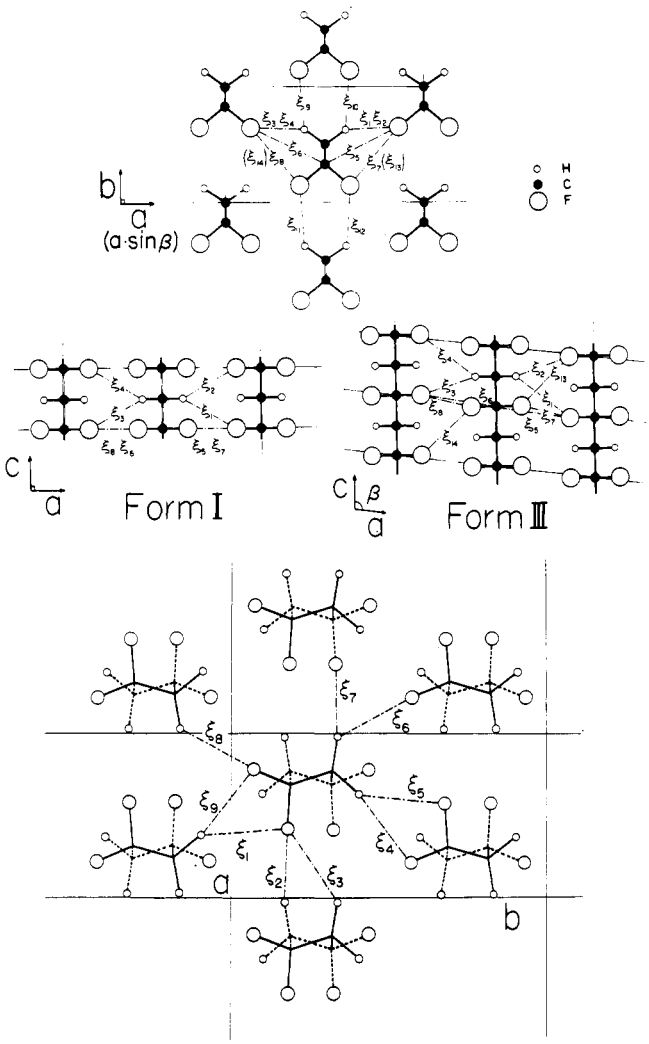

Figure 5. Crystal structures and intermolecular interactions in the three crystal forms of poly(vinylidene fluoride): (top) forms I and III, (bottom) form II.

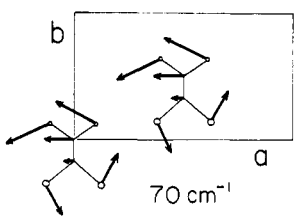

Figure 6. Schematical representation of the librational lattice mode of crystal form I of poly(vinylidene fluoride).

ed as due to the optically active vibrational modes of the regular crystal of form I. However, there are many observed additional weak bands in the spectra as found in Figure 2. Moreover, on cooling to liquid nitrogen temperature the infrared band due to the librational lattice mode shifts to the higher frequency side and splits into at least two components with the peaks at 86 and 76 (shoulder) cm^{-1} (Figure 7). Very small amounts of splittings are also observed for the infrared bands in the higher frequency region (Figure 8). These facts are in conflict with the regular *Cm2m* crystal structure, since the spectroscopic unit cell contains only one chain. Therefore, we may suppose some kind of disordered structure as the origin of the observed band splittings and of appearance of additional weak bands. This problem will be discussed in detail in a later section.

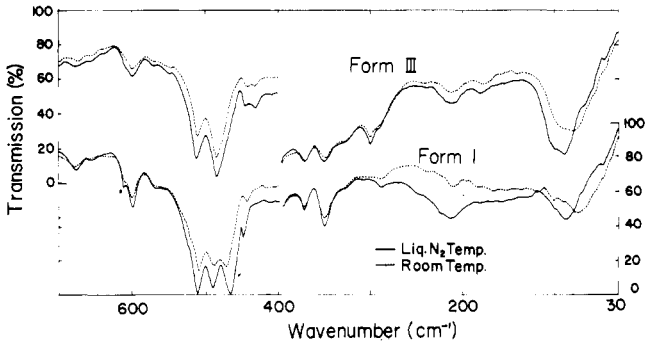

Figure 7. Infrared spectra of crystal forms I and III of poly(vinylidene fluoride) measured at room (- - -) and liquid-nitrogen (——) temperature.

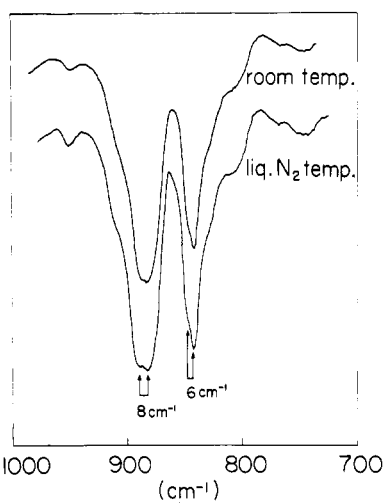

Figure 8. Splitting of the infrared absorption bands of crystal form I of poly(vinylidene fluoride) measured on cooling to liquid-nitrogen temperature (powder sample).

Structure and Vibrations of Crystal Form III

The crystal structure of form III proposed by the authors[2] belongs to a monoclinic system with the space group $C121\text{-}C_2^3$, containing two planar zigzag chain with slight deflection as in form I. The crystal lattices of forms I and III differ from each other in the relative height of the two chains in the unit cell as shown in Figure 5. If we ignore the deflection of the chain, the crystal lattice of form III gives rise to the optically active modes given in Table IV. As in the case of form I, only one librational lattice mode (B species) is expected in both infrared and Raman spectra. Comparing Tables IV(a) and IV(b), we can see that the A_1 and A_2 modes of form I correspond to the A modes of form III, and the B_1 and B_2 modes of form I to the B modes of form III. Apart from infrared activity of the A_2 species, to which the CH_2 and CF_2 twisting modes belong, similar vibrational modes occur in both crystal forms. There are, however, distinct differences in the observed spectra between two forms.

In order to interpret the spectral differences between forms I and III, the normal frequencies of form III were calculated to be compared with those of form I. The calculation was made on a monoclinic lattice with the same size of c projection ($a' = a \sin \beta = 8.58$ Å, $b = 4.91$ Å) as form I, but with the angle of $\beta = 97°$ different from the orthorhombic lattice ($\beta = 90°$) of form I. The molecules in the lattice were assumed to have the same bond lengths, valence angles, torsional angles (planar zigzag), and fiber period (2.56 Å) as those in form I. Although this crystal lattice differs slightly from that proposed by the previous X-

Table V
Observed and Calculated Frequencies and Potential Energy Distribution (PED) of Crystal Forms I and III of Poly(vinylidene fluoride)

Form I						Form III						
	Frequencies, cm^{-1}						Frequencies, cm^{-1}					
	Obsd						Obsd					
Species	Infrared		Raman		Calcd	Species	Infrared		Raman		Calcd	PED (%)[c]
A_1	2980 (⊥)[a]	vw[b]	2984	s	2980	*A*	2980 (⊥)	vw	2984	s	2987	$\nu_s(CH_2)$[d] (99)
	1428 (⊥)	w	1436	s	1423		1427 (⊥)	w	1434	vs	1430	$\delta(CH_2)$ (81)
	1273 (⊥)	s	1283	m	1286		1269 (⊥)	w	1270	m	1287	$\nu_s(CF_2)$ (40) − $\nu_s(CC)$ (22) + $\delta(CCC)$ (15)
	884 (⊥)	s	886	s	879		882 (⊥)	s	884	s	880	$\nu_s(CF_2)$ (54) + $\nu_s(CC)$ (18)
	508 (⊥)	s	514	m	508		510 (⊥)	s	516	m	510	$\delta(CF_2)$ (98)
A_2	Inactive		980	w	983		950 (–)	vw	942	w	982	$t(CH_2)$ (100)
			268	m	262		270 (–)	vw	268	m	262	$t(CF_2)$ (100)
B_1	1398 (∥)	s	1400	w	1396	*B*	1400 (∥)	s	1397	w	1396	$w(CH_2)$ (58) − $\nu_a(CC)$ (35)
	1071 (∥)	m	1078	m	1065		1073 (∥)	w	1078	m	1065	$\nu_a(CC)$ (54) − $w(CF_2)$ (22) + $w(CH_2)$ (24)
	468 (∥)	s	475	w	470		483 (∥)	vs	487	m	473	$w(CF_2)$ (92)
B_2	3022 (⊥)	vw	3020	vs	3029		3020 (⊥)	vw	3020	vs	3036	$\nu_a(CH_2)$ (99)
	1176 (⊥)	s	1175	w	1182		1175 (⊥)	s	1178	m	1182	$\nu_a(CF_2)$ (64) − $r(CF_2)$ (21) + $r(CH_2)$ (15)
	840 (⊥)	s	845	vs	825		838 (⊥)	m	843	vs	825	$r(CH_2)$ (60) − $\nu_a(CF_2)$ (31)
	442 (⊥)	w	445	w	443		440 (⊥)	w	437	m	458	$r(CF_2)$ (74) + $r(CH_2)$ (26)
	70 (⊥)	s	77	w	72		84 (–)	s			106	Librational lattice mode

[a] Infrared dichroism: ⊥, electric vector perpendicular to the orientation direction; ∥, electric vector parallel to the orientation direction. [b] Relative intensity; vs, very strong; s, strong; m, medium; w, weak; vw, very weak. [c] The values obtained by the normal coordinate treatment for a single chain. [d] Symmetry coordinates; ν_s, symmetric stretching; ν_a, antisymmetric stretching; δ, bending; w, wagging; t, twisting; r, rocking. The sign + or − denotes the phase relation among the symmetry coordinates.

ray analysis, it is more convenient for the present purpose to investigate the spectral changes originated from the differences in packing of the molecular chains. The intramolecular forces were the same as those of form I, and the intermolecular force constants which vary with the interatomic distances were deduced by using the same potential function as used for form I. The calculated frequencies of form III are given in Table V.

The librational lattice mode of form III appears as an infrared absorption having a peak at 84 cm^{-1}, about 14 cm^{-1} higher than that in form I. The calculated normal frequency (106 cm^{-1}) of the mode is consistent with the observed tendency. The CF_2 bending $\delta(CF_2)$, wagging $w(CF_2)$, and rocking $r(CF_2)$ modes appear around 500 cm^{-1} in the infrared spectrum. In this region distinct spectral differences are observed between forms I and III as shown in Figure 2. The bands due to the $\delta(CF_2)$ and $w(CF_2)$ modes in form III appear at frequencies higher than those in form I. The calculated frequencies of these modes are consistent with the observed tendency as shown in Table V. The perpendicular band at 442 cm^{-1} in form I is assigned to the $r(CF_2)$ mode. The corresponding band in form III is rather obscure. The diffuse absorption with two peaks at 440 and 431 cm^{-1} in form III is possibly assigned to the $r(CF_2)$ mode. We have, however, some doubt about the assignment because the calculated frequency of the mode is higher in form III than in form I, in contrast to the observed result. As another possibility, the absorption may correspond to a peak of the frequency distribution function which will be dealt with in the next section.

It should be noticeable that form III gives higher frequency for the librational lattice mode as well as the CF_2 deformations as compared with form I, reflecting stronger intermolecular forces in form III than in form I. The heights along the chain axis of the two chains in the monoclinic unit cell of form III differ from each other by 0.53 Å, while they are on the same height in the orthorhombic cell of form I. In form III the shortest H···F distance (ξ_2 and ξ_4) of 2.43 Å (corresponding to the largest intermolecular force constant of 0.0657 mdyn/ Å) is 0.21 Å shorter than the corresponding H···F distance in form I. The force constant due to the shortest H···F distance in form I ($\xi_1 - \xi_4$) is 0.0163 mdyn/Å, quite a bit smaller than in form III. The number of the shortest atomic pairs in form I is, however, twice as much as in form III because of the mirror symmetry perpendicular to the *c* axis in the orthorhombic cell. Therefore, the resultant intermolecular forces in the two crystal forms are not so much different from each other (see Table III).

Thus, the differences in vibrational spectrum between forms I and III are interpreted fairly well by the crystal structures proposed previously by means of X-ray analysis. Therefore, form III should be regarded as the third crystal phase independent of form I.

The profiles of the infrared absorption curve around 1250 cm^{-1} and of the Raman scattering curve around 810 cm^{-1} show a remarkable difference between forms I and III. The corresponding peaks or shoulders appear at similar frequencies, but the relative intensities, especially those of the infrared bands at 1273 and 1230 cm^{-1} and of the Raman band at 810 cm^{-1}, are quite different from each other in the two crystal forms. In form III the 1230-cm^{-1} band is stronger than the 1273-cm^{-1} band which is assigned to the A_1 fundamental in form I. It may be possible to assign the former to the A fundamental of form III instead of the latter. However, such a big frequency difference for the same molecular mode in the two crystal forms cannot be reproduced by the present calculation. As will be

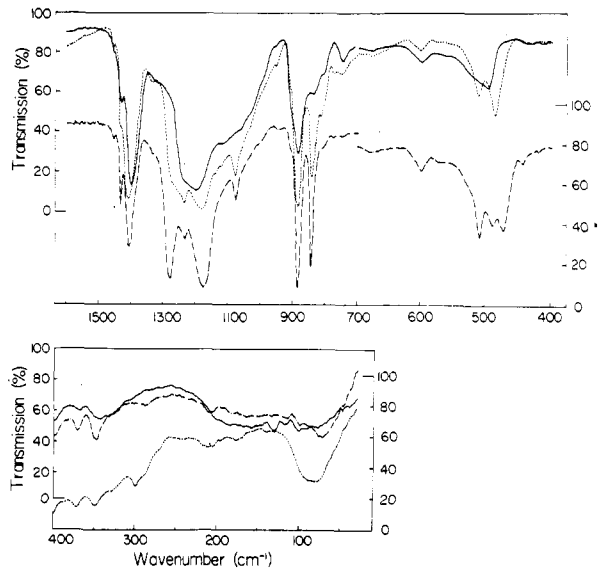

Figure 9. Infrared spectra of molten sample (——), compared with those of form I (— · —) and form III (· · ·) of poly(vinylidene fluoride).

discussed later, it seems that vibrations of the noncrystalline region play a great role in the spectra of these regions.

At liquid nitrogen temperature the absorption due to the librational lattice mode of form III shows a peak at 89 cm^{-1} with distinct shoulders at 98 and 68 cm^{-1} (Figure 7). The absorption bands in higher frequency regions show small amounts of splitting at low temperature as in the case of form I. Moreover, many weak infrared and Raman bands appear throughout the whole frequency range of the spectra in addition to the strong bands due to the optically active fundamentals. The origins of these bands will be discussed in the next section.

Frequency Distribution Function and Disordered Structure in Crystal Forms I and III

As mentioned in the preceding two sections the infrared and Raman spectra of forms I and III have many bands which are not assigned to the optically active fundamentals. Most of them are crystalline bands since they disappear in molten sample (Figure 9), suggesting disordered structures present in the crystalline region of these two forms.

In a disordered crystal lattice without translational symmetry among the unit cells, the selection rules of the regular lattice are broken down and, therefore, all the vibrational modes with any value of the wavenumber vector **k** contribute, in principle, to the vibrational spectra. In general, the defects involved in the crystal lattice give rise to some changes in the vibrational modes of the regular lattice. When the effect of the disordered structure on the vibrational modes is not so serious, we may compare the observed spectra of a disordered lattice with the frequency distribution function computed for the corresponding regular lattice, except for the so-called localized modes in which the molecular motions are localized in a certain disordered domain.

The normal frequencies of the modes in the first Brillouin zone were calculated at the interval of $\pi/5$ for δ_a and δ_b and $\pi/20$ for δ_c, and the dispersion relations with respect to δ_c were drawn for each combination of (δ_a, δ_b). Here, δ_a, δ_b, and δ_c denote the phase difference along the *a*, *b*, and *c* axis, respectively. The dispersion curves for (0, 0, δ_c) are shown in Figure 10. In the case of form I the (0, 0, δ_c) modes have the space group symmetry isomorphous to the

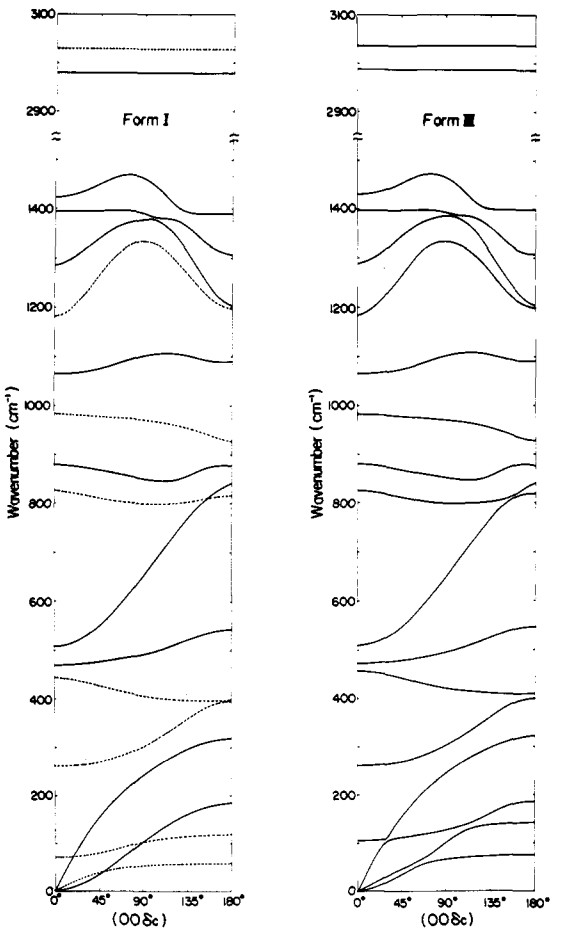

Figure 10. Dispersion relations of poly(vinylidene fluoride) crystals: (left) form I, (——) in-plane modes, (· · ·) out-of-plane modes; (right) form III.

point group C_s, except for the modes at the point of (0, 0, 0) (the Γ point) having the factor group symmetry of C_{2v}. Therefore, the branches are divided into two kinds of mode: the in-plane and out-of-plane modes as represented by the solid and broken lines, respectively, in the figure. In the case of form III the (0, 0, δ_c) branches belong to C_1 symmetry and therefore every branch interacts with others.

The frequency distribution functions $g(\nu)$ of forms I and III were constructed by measuring the lengths of the line segments contained in each frequency range divided by the step height of 5 cm^{-1} in the dispersion curves. The difference in crystal structure between forms I and III is reflected on clear difference in the dispersion relations for the acoustic branches as well as the low-frequency optical branches. The frequency distribution functions of forms I and III are compared with each other in Figure 11. Here the infrared absorption curves are described for comparison. The single peak at 400 cm^{-1} in $g(\nu)$ of form I splits into two peaks at 400 and 420 cm^{-1} in form III. The latter may correspond to the weak absorptions around 430 cm^{-1} as stated in the preceding section.

In Figure 12 the frequency distribution function of form I is compared with the observed infrared spectrum. The positions of the Raman lines are also indicated at the top of the figure. It should be noted here that the height of the peaks in $g(\nu)$ should not necessarily be related to the infrared or Raman intensity, and the peaks indicate only the positions where the normal frequencies are concentrated. The broken lines indicate the frequencies of the optically active modes with **k** = 0, and they correspond well to the strong absorptions (or to the strong Raman lines for the A_2

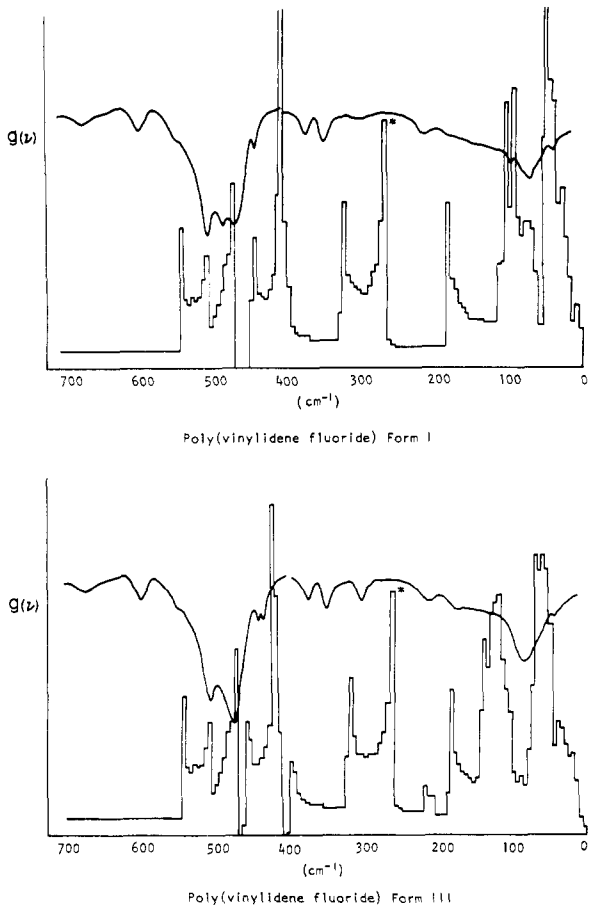

Figure 11. Frequency distribution functions in the far-infrared region of poly(vinylidene fluoride) crystals: (top) form I, (bottom) form III. The solid lines represent the observed infrared absorption curves.

modes marked with an asterisk). It is a characteristic of $g(\nu)$ that some of the peaks of $g(\nu)$ appear around the positions of the $\mathbf{k} = 0$ modes. The other peaks of $g(\nu)$ are associated with the weak bands or shoulders of the infrared spectrum as shown in Figure 12.

Thus, most of the weak absorptions, which are not assigned to the optically active modes of the regular lattice, are attributed to some kind of disorder involved in the crystal lattices. First we are concerned with the disorder in the molecular structure. From the dispersion relations (Figure 10) we can recognize that most of the peaks of $g(\nu)$ corresponding to the weak absorptions appear at the positions close to the molecular modes with $\delta_c = \pi$. These molecular modes are of course inactive in the vibrational spectra for the fully extended zigzag chain. They become active if the molecular chain twists alternately from the planar structure. Therefore, the appearance of these modes in the spectra may be related to the slightly deflected structure of the chains proposed by the previous X-ray work.[2]

In addition to the disorder in molecular structure, some disordered packing of the chains in the crystal lattice may be supposed from the good correspondence between the infrared absorption profile and the frequency distribution function in the region of lattice vibration (Figure 12). The splittings found for some infrared bands at low temperature are also ascribed to the same origin.

There are absorptions which are associated with neither the optically active modes nor the peaks of the frequency distribution function. Some of them are due to the disorders in molecular conformation, for example, the gauche form involved in the noncrystalline phase. The infrared

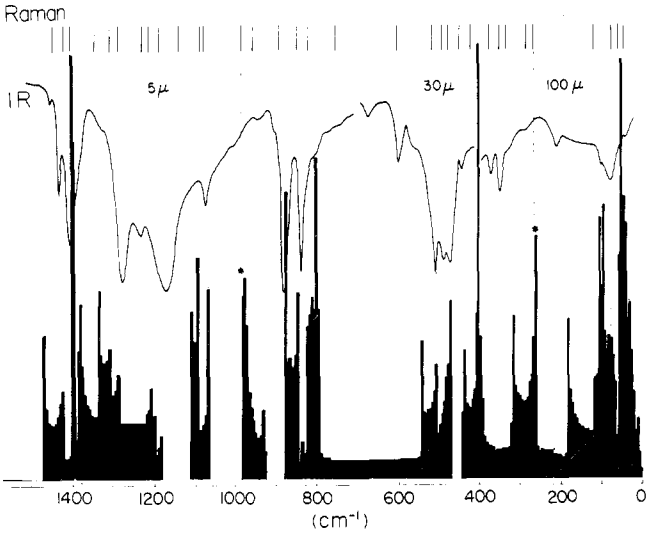

Figure 12. Frequency distribution function of crystal form I of poly(vinylidene fluoride). The solid curves represent the observed infrared absorption and the vertical lines at the top denote the positions of the Raman lines.

band at 489 cm^{-1} in form I which increases the intensity in the molten state (200°) may belong to this category (Figure 9). In fact, there appears a strong band at 489 cm^{-1} in the spectrum of form II including the gauche form in the molecule. The 600-cm^{-1} band may be due to the noncrystalline part because it appears in the infrared spectra of the three crystal forms as well as in the melt, and there are no peaks in $g(\nu)$ corresponding to the band. In the infrared spectrum of the molten sample there is a strong and broad absorption around 1230 cm^{-1}. In partially crystalline samples this amorphous band overlaps the crystalline bands in this region and changes the spectral feature depending on the degree of crystallinity of the sample. The spectral difference in this region between forms I and III may be due partly to the difference in fine structure between the crystal phases.

Another kind of disordered structure in PVDF concerns the head-to-head linkages. From nmr studies the sample of PVDF used here contains about 10% head-to-head linkages ($CH_2CF_2CF_2CH_2$) immediately followed by tail-to-tail linkages ($CF_2CH_2CH_2CF_2$)

$$CH_2CF_2CH_2CF_2CF_2CH_2CH_2CF_2CH_2CF_2$$

In order to investigate the vibrational modes associated with this chemical structure, vibrational analysis was made for the alternating copolymer of ethylene and tetrafluoroethylene as a typical model compound consisting of this chemical structure. The polarized infrared and the Raman spectra of the copolymer are reproduced in Figure 13.

From the fiber period of 5.08 Å the molecule is considered to assume planar zigzag conformation in the crystalline region. The normal modes of the molecule can be treated with the factor group isomorphous to the point group C_{2h}. The result of the factor group analysis is given in Table VI. In the normal modes calculation the following molecular parameters are assumed: C–H, 1.09 Å; C–F, 1.34 Å; C–C, 1.54 Å; all the valence angles, 109°28′. The VFF force constants are listed in Table VII. The calculated normal frequencies are compared with the observed data in Table VIII.

The strong infrared absorptions at 1453 ($\perp$), 1323 ($\parallel$), and 666 ($\parallel$) cm^{-1} of the copolymer seem to be characteristic of the head-to-head or tail-to-tail structure, because around these frequencies there are no optically active fundamentals of the PVDF molecules of both TT (forms I and

Table VI
Number of the Normal Modes and Selection Rules for a Planar Zigzag Molecule of the Alternating Copolymer of Ethylene and Tetrafluoroethylene with C_{2h} Symmetry

Species	Molecular modes	Ingenuine vibrations[a]	Selection rules: Infrared	Selection rules: Raman
A_g	10		Forbidden	Active
B_g	7	R_c	Forbidden	Active
A_u	7	T_a	Active ($\perp$)[b]	Forbidden
B_u	8	T_c, T_b	Active ($\perp$, $\parallel$)	Forbidden

[a] R_c, pure rotation around the fiber axis; T_a, pure translation along the direction perpendicular to the molecular plane; T_b, pure translation in the molecular plane along the direction perpendicular to the fiber axis; T_c, pure translation along the fiber axis. [b] $\perp$ and $\parallel$ in parentheses denote infrared polarization for a uniaxially oriented specimen.

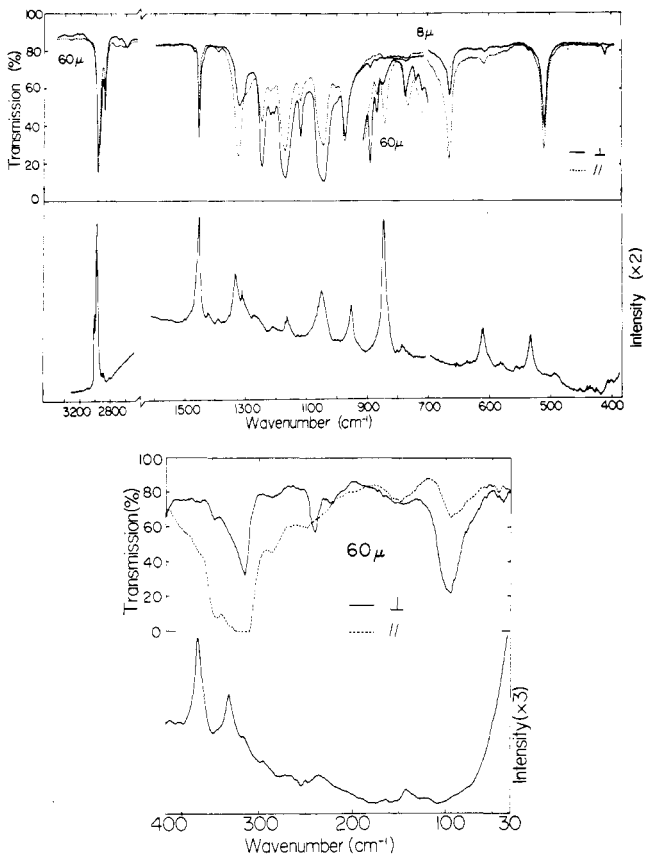

Figure 13. Infrared (upper) and Raman (lower) spectra of the alternating copolymer of ethylene and tetrafluoroethylene in the region (top) from 4000 to 400 cm^{-1}, and (bottom) below 400 cm^{-1}. For infrared absorption: (——) electric vector $\perp$ orientation direction; (- - -) electric vector $\parallel$ orientation direction.

III) and TGTḠ (form II) conformations. In the infrared spectra of the three crystal forms and the molten sample of PVDF there appear weak absorptions around the three frequencies mentioned above: 1450, 1320–1340, and 678 cm^{-1}. They may be due to the head-to-head linkages involved in the sample of PVDF. It is noticeable that these bands show rather clear dichroism and become stronger and sharper by annealing the sample. This suggests that the head-to-head units in PVDF may be accommodated in the crystalline region, consistent with the conclusion proposed by Doll and Lando[16] by means of thermal analysis and X-ray diffraction.

Then, assuming that the head-to-head units cocrystallize

Table VII
Intramolecular Valence Force Constants of the Alternating Copolymer of Ethylene and Tetrafluoroethylene

No.	Force constants	Coordinates involved	Common atoms	Values[a]
1	K_d	CH		4.833
2	K_R	CC		3.963
3	F_{R1}	CC, CF	C	0.448
4	F_R	CC, CC	C	0.148
5	$F_{R\gamma}$	CC, CCH	CC	0.233
6	$F_{R\omega}$	CC, CCC	CC	0.492
7	$F_{R\phi}$	CC, CCF	CC	0.575
8	F_d	CH, CH	C	0.076
9	K_1	CF		6.597
10	F_{11}	CF, CF	C	0.683
11	$F_{1\xi}$	CF, CFF	CF	0.671
12	H_γ	CCH		0.765
13	F_γ	CCH, CCH	CC	0.079
14	F_γ'	CCH, CCH	CH	0.230
15	H_δ	CHH		0.443
16	H_ω	CCC		0.942
17	$f_\omega{}^t$	CCC, CCC(t)	CC	0.166
18	H_ϕ	CCF		1.381
19	H_ξ	CFF		1.225
20	T	CCCC		0.149
21	$F_{1\phi}$	CF, CCF	CF	0.554
22	F_ϕ	CCF, CCF	CC	0.259
23	F_ϕ'	CCF, CCF	CF	0.037
24	$f_{\omega\gamma}{}^g$	CCC, CCH(g)	CC	0.146
25	$f_{\omega\phi}{}^g$	CCC, CCF(g)	CC	0.012
26	$f_{\gamma\phi}{}^t$	CCH, CCF(t)	CC	0.046
27	$f_{\gamma\phi}{}^g$	CCH, CCF(g)	CC	0.403
28	$f_\gamma{}^t$	CCH, CCH(t)	CC	−0.071
29	$f_\gamma{}^g$	CCH, CCH(g)	CC	0.018
30	$f_\phi{}^t$	CCF, CCF(t)	CC	0.095
31	$f_\phi{}^g$	CCF, CCF(g)	CC	−0.054
32	$F_{d\gamma}$	CCH, CH	CH	0.041
33	$F_{R\gamma}$	CCH, CC	CC	0.233
34	$F_{d\delta}$	CHH, CH	CH	−0.132

[a] The stretch constants have units of mdyn/Å; the stretch-bend interactions have units of mdyn/rad; and the bending constants have units of (mdyn Å)/rad^2.

in planar zigzag structure with the homopolymer parts, we examined the vibrational modes of these units by calculating the normal vibrations of such molecules as

$$[-(CH_2CF_2)_mCF_2CH_2-]$$

where m varies from two to four. Since the above three bands are found to be due to the CH_2 bending, the CH_2 wagging, and the CF_2 wagging modes, respectively, from the vibrational analysis of the alternating copolymer (m = 1) (Table VIII), we focused our attentions on these three modes. For the above three molecular models the vibrational frequencies and the **L** vectors are calculated by using the same molecular parameters and force constants as those of the alternating copolymer. Among these normal modes the vibrations are picked up which contain considerable amounts of the contribution from the head-to-head or tail-to-tail chemical groups. In Figure 14 are summarized the results of the normal mode calculations along with the results of the alternating copolymer. Here are given the potential energy distributions (relative values) among the CH_2 (represented with ○) or CF_2 (●) groups along the chain, the schematical representations (in terms of the **L**-vector elements) of the characteristic vibrational modes,

Table VIII
Observed and Calculated Frequencies and Potential Energy Distribution (PED) of the Alternating Copolymer of Ethylene and Tetrafluoroethylene

Species	Frequencies, cm^{-1} Obsd Infrared	Obsd Raman	Calcd	PED (%)
A_g	Inactive	2979 vs[a]	2969	$\nu_s(CH_2)$[c] (99)
		1453 s	1441	$\delta(CH_2)$ (84)
		1330 m	1333	$\nu'(CC)$ (15) + $w(CH_2)$ (45)
		1163 w	1189	$\nu_s(CF_2)$ (47) + $\delta(CCC)$ (19)
		1050 m	1028	$\nu(CC)$ (37) + $w(CF_2)$ (28) + $w(CH_2)$ (17)
		952 m	966	$\nu'(CC)$ (62) − $w(CH_2)$ (21)
		845 s	836	$\nu_s(CF_2)$ (25) + $\nu_s(CC)$ (40) − $\delta'(CCC)$ (32)
		610 m	590	$\nu(CC)$ (16) + $\delta(CF_2)$ (32) − $\delta(CCC)$ (18)
		369 m	378	$\delta(CF_2)$ (72)
		240 vw	219	$\delta(CCC)$ (30) − $\delta'(CCC)$ (34) + $w(CF_2)$ (29)
B_g	Inactive	3005 s	2989	$\nu_a(CH_2)$ (99)
		1310 m	1321	$\nu_a(CF_2)$ (65) − $r(CF_2)$ (28)
		1070 sh	1066	$r(CH_2)$ (79)
			943	$t(CH_2)$ (85) + $r(CH_2)$ (15)
		530 m	526	$\nu_a(CF_2)$ (18) + $r(CF_2)$ (69)
		337 m	321	$t(CF_2)$ (62) − $r(CF_2)$ (19)
		145 w	135	τ_1(87)
A_u	2956 (⊥)[b] vw	Inactive	2985	$\nu_a(CH_2)$ (100)
	1245 (⊥) s		1245	$\nu_a(CF_2)$ (86)
	1045 (⊥) s		1038	$t(CH_2)$ (98)
	890 (⊥) w		884	$r(CH_2)$ (92)
	410 (⊥) vw		434	$t(CF_2)$ (39) − $r(CF_2)$ (36)
	240 (⊥) m		230	$t(CF_2)$ (53) + $r(CF_2)$ (41)
	98 (⊥) s		91	$\tau_2(34) - \tau_3(34)$ + $r(CF_2)$ (24)
B_u	2975 (∥) vw	Inactive	2976	$\nu_s(CH_2)$ (99)
	1453 (⊥) s		1466	$\delta(CH_2)$ (94)
	1323 (∥) s		1324	$w(CH_2)$ (79)
	1169 (⊥) s		1148	$\nu_s(CF_2)$ (72)
	976 (∥) s		970	$\nu_a(CC)$ (48) − $w(CF_2)$ (29) + $w(CH_2)$ (18)
	666 (∥) s		682	$\nu_a(CC)$ (28) + $w(CF_2)$ (40)
	508 (∥) s		510	$\delta(CF_2)$ (87)
	316 (∥) vs		306	$\delta(CCC)$ (34) + $\delta'(CCC)$ (33) + $w(CF_2)$ (25)

[a] Relative intensity: vs, very strong; s, strong; m, medium; w, weak; vw, very weak; sh, shoulder. [b] Infrared dichroism: ⊥, electric vector perpendicular to the orientation direction; ∥, electric vector parallel to the orientation direction. [c] Symmetry coordinates: ν_s, symmetric stretching; ν_a, antisymmetric stretching; δ, bending, w, wagging; t, twisting; r, rocking; ν(CC), stretching of the C(F)-C(F) bond; ν'(CC), stretching of the C(H)-C(H) bond; ν_s(CC), symmetric stretching of two C(H)-C(F) bonds; ν_a(CC), antisymmetric stretching of two C(H)-C(F) bonds; δ (CCC), skeletal bending of C(F)-C(H)-C(F); δ'(CCC), skeletal bending of C(H)-C(F)-C(H); τ_1, symmetric combination of two torsional modes of C(F)-C(F)-C(H)-C(H); τ_2, torsional mode of C(F)-C(H)-C(H)-C(F); τ_3, torsional mode of C(H)-C(F)-C-(F)-C(H). The sign + or − denotes the phase relation among the symmetry coordinates.

and their vibrational frequencies which vary more or less depending on the head-to-head or tail-to-tail contents.

(a) The CH_2 bending mode of the tail-to-tail, CH_2CH_2, units. The atomic displacements of the mode are almost localized on the CH_2CH_2 groups and the frequency (1473 cm^{-1}) does not depend on the value of m, exerting little coupling with other modes. Therefore, this is clearly a localized mode characteristic of the tail-to-tail units. Since the frequency lies within the band area of the $\delta(CH_2)$ dispersion curve of PVDF homopolymer (form I) (see Figure 10), this mode belongs to the so-called "in-band localized mode."[17]

(b) The CH_2 wagging mode of the tail-to-tail units. This is also an in-band localized mode due to the CH_2CH_2 groups with the frequency in the range of 1320–1335 cm^{-1} depending on the amount of the tail-to-tail units involved. The skeletal stretchings couple with this mode.

(c) The CF_2 wagging mode of the head-to-head, CF_2CF_2, units. The behavior of the mode is rather complicated as compared with the above two cases. For a small value of m

Table IX
Number of the Normal Modes and Selection Rules of Poly(vinylidene fluoride) Form II with Space Group $P2_1/c$-C_{2h}^5

Species	Molecular modes	Lattice modes	Selection rules: Infrared	Selection rules: Raman
A_g	16	$L(T_a)$,[a] $L(T_c)$	Forbidden	Active
B_g	16	$L(T_b)$, $L(R_c^0)$[b]	Forbidden	Active
A_u	16	T_b,[c] $L(R_c^\pi)$	Active (⊥)[d]	Forbidden
B_u	16	T_a, T_c	Active (⊥, ∥)	Forbidden

[a] $L(T_a)$, $L(T_b)$, $L(T_c)$: translational lattice modes. [b] $L(R_c^0)$, $L(R_c^\pi)$: librational lattice modes around the fiber axis with the phase difference of 0 and π between the two chains in the unit cell, respectively. [c] T_a, T_b, T_c: pure translation along the respective crystal axis. [d] ⊥ and ∥ in parentheses denote infrared polarization for a uniaxially oriented specimen.

Table X
Observed and Calculated Frequencies and Potential Energy Distribution (PED) of Poly(vinylidene fluoride) Form II

Species	Frequencies, cm^{-1} Obsd Infrared		Obsd Raman		Calcd	PED (%)[a]
B_u	3017 (⊥)[b]	w[c]			3042	$\nu_a(CH_2)$[d] (99)
A_g			2990	s	3042	
B_u	2977 (⊥)	w			2975	$\nu_s(CH_2)$ (99)
A_g			2970	sh	2975	
B_u	1420 (⊥)	m			1456	$\delta(CH_2)$ (54) − $w(CH_2)$ (31)
A_g			1430	s	1455	
B_u	1399 (∥)	s			1392	$\delta(CH_2)$ (29) + $w(CH_2)$ (29) − $\nu_a(CC)$ (24)
A_g			1406	vw	1392	
B_u	1290 (∥)	w			1278	$\nu_a(CF_2)$ (53) − $r(CF_2)$ (15)
A_g			1296	m	1279	
B_u	1149 (∥)	m			1159	$\nu_a(CC)$ (30) − $\nu_s(CF_2)$ (24)
A_g			1150	w	1158	
B_u	1056 (∥)	m			1083	$\nu_s(CF_2)$ (35) + $w(CH_2)$ (17)
A_g			1058	m	1083	
B_u	976 (⊥)	w			975	$t(CH_2)$ (82)
A_g			976	w	973	
B_u	873 (⊥)	s			877	$\nu_s(CC)$ (38) + $\delta(CCC)$ (22)
A_g			876	s	880	
B_u	853 (⊥)	w			835	$r(CH_2)$ (48)
A_g			841	m	834	
B_u	612 (∥)	s			621	$\delta(CF_2)$ (24) − $\delta'(CCC)$ (19)
A_g			612	s	617	
B_u	489 (∥)	s			509	$\delta(CF_2)$ (48) + $w(CF_2)$ (25)
A_g			488	m	513	
B_u	410 (∥)	vw			423	$r(CF_2)$ (53) + $r(CH_2)$ (19)
A_g			414	s	434	
B_u	288 (∥)	s			309	$t(CF_2)$ (54) + $w(CF_2)$ (18)
A_g			287	s	304	
B_u	208 (∥)	m			247	$t(CF_2)$ (38) − δ (CCC) (19) + $\delta'(CCC)$ (18)
A_g			206	w	231	
B_u	100 (⊥)	m			94	$\tau_a(28) + \tau_s(23) + \delta(CCC)$ (20) + $r(CF_2)$ (18)
A_g			75	w	77	
A_g			52	w	59	$L(T_a)$
A_g			29	w	11	$L(T_c)$
A_u	3017 (⊥)	w			3040	$\nu_a(CH_2)$ (100)
B_g			3030	s	3040	
A_u	2977 (⊥)	w			2977	$\nu_s(CH_2)$ (99)
B_g			2980	sh	2977	
A_u					1477	$\delta(CH_2)$ (49) − $w(CH_2)$ (28)
B_g			1442	sh	1477	
A_u	1383 (⊥)	m			1359	$\delta(CH_2)$ (39) + $w(CH_2)$ (22)
B_g			1384	vw	1360	
A_u	1209 (⊥)	s			1241	$\nu_a(CF_2)$ (41) + $w(CH_2)$ (26)
B_g			1200	m	1241	
A_u	1182 (⊥)	s			1199	$\nu_s(CF_2)$ (39) + $t(CH_2)$ (16)
B_g			1190	sh	1198	
A_u	1067 (⊥)	m			1069	$\nu_s(CC)$ (65)
B_g			1064	sh	1069	
A_u					934	$t(CH_2)$ (60) − $\nu_a(CF_2)$ (21)
B_g			940	vw	935	
A_u	878 (⊥)	s			918	$\nu_a(CC)$ (60) + $\nu_s(CF_2)$ (20)
B_g			885	sh	917	
A_u	795 (⊥)	w			818	$r(CH_2)$ (78)
B_g			800	vs	815	
A_u	766 (⊥)	m			774	$\delta(CF_2)$ (33) + $\delta(CCC)$ (21)
B_g			766	w	776	
A_u	531 (⊥)	w			529	$\delta(CF_2)$ (52)
B_g			536	m	528	

Table X *(Continued)*

Species	Frequencies, cm^{-1} Obsd Infrared	Obsd Raman	Calcd	PED (%)[a]
A_u	389 (⊥) vw		407	r(CF_2) (52)
B_g			398	
A_u	355 (⊥) s		372	t(CF_2) (63) + r(CF_2) (16)
B_g		357 vw	371	
A_u	215 (⊥) s		283	δ(CCC) (33) + δ′(CCC) (28) + r(CF_2) (15)
B_g		216 sh	283	
A_u	176 (⊥) w		120	τ_a(71)
B_g		176 w	130	
A_u	53 (⊥) w		51	L(R_c^{τ})
B_g		99 w	84	L(T_b)
B_g			62	L(R_c^{0})

[a] The values calculated by the normal coordinate treatment for a single chain of TGTḠ conformation with C_s symmetry. [b] Infrared dichroism: ⊥, electric vector perpendicular to the orientation direction; ∥, electric vector parallel to the orientation direction. [c] Relative intensity: vs, very strong; s, strong; m, medium; w, weak; vw, very weak; sh, shoulder. [d] Symmetry coordinates: ν_s, symmetric stretching; ν_a, antisymmetric stretching; δ, bending; w, wagging; t, twisting; r, rocking; δ(CCC), skeletal bending of C(F)-C(H)-C(F); δ′(CCC), skeletal bending of C(H)-C(F)-C(H); τ_s, symmetric combination of two torsional modes of C(H)-C(F)-C(H)-C(F); τ_a, antisymmetric combination of two torsional modes of C(H)-C(F)-C(H)-C(F). The sign + or − denotes the phase relation among the symmetry coordinates.

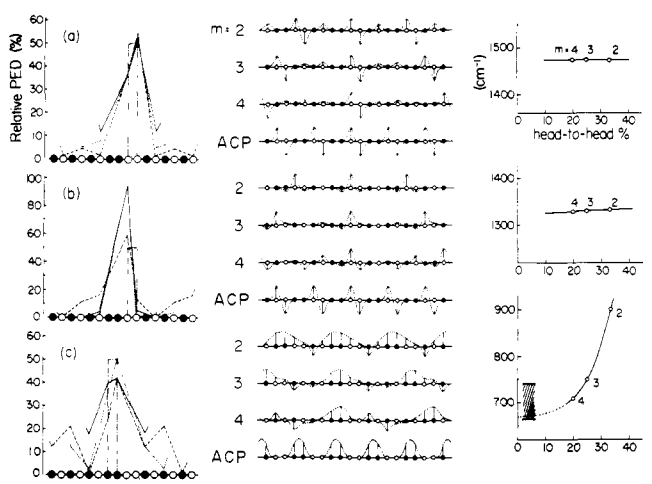

Figure 14. The calculated normal vibrations of the head-to-head or tail-to-tail units: (a) CH_2 bending, (b) CH_2 wagging, and (c) CF_2 wagging modes. From left to right, PED, **L** vectors, and frequency changes of four molecular models of [-(CH_2CF_2)$m$$CF_2CH_2$-] [$m$ = 1 (alternating copolyer, ACP), 2, 3, and 4]. ● and ○ represent the CF_2 and CH_2 groups, respectively. In PED: (——) m = 2; (· · ·) m = 3; (- - -) m = 4; (— - —) ACP.

this mode includes appreciable contribution from the wagging modes of all the CF_2 groups in the molecule. The frequency of the mode is strongly dependent upon the amount of the head-to-head content. As m increases the atomic displacements tend to concentrate on the CF_2CF_2 groups and the frequency goes asymptotically to about 670 cm^{-1}. The dispersion curve associated with the w(CF_2) mode of the CF_2CF_2 groups of the alternating copolymer (Figure 15) is limited within the frequency range of 660–740 cm^{-1} as indicated by the hatched area in Figure 14c. The frequency of 670 cm^{-1} is, therefore, recognized as the characteristic frequency of the head-to-head units, and the infrared band at 678 cm^{-1} observed in the commercial PVDF samples is thought to be a "pseudo-localized band"[18] which occurs for the case of a small number of defects in a low density frequency region of the perfect homopolymer (see Figure 12). This w(CF_2) mode highly couples with the skeletal stretching modes.

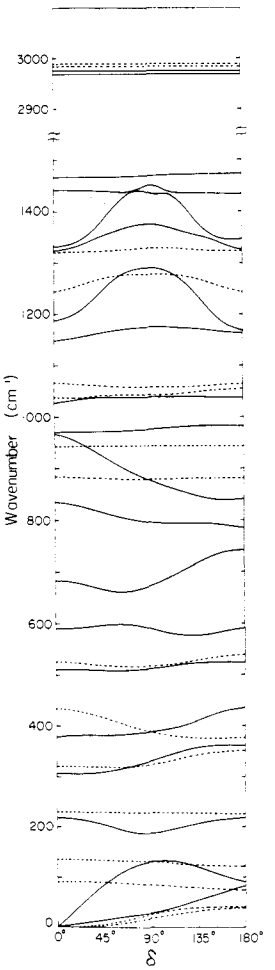

Figure 15. Dispersion relations for a single chain of the alternating copolymer of ethylene and tetrafluoroethylene: (——) in-plane modes; (- - -) out-of-plane modes.

From the above discussions the infrared bands at 1450, 1320–1340, and 678 cm^{-1} of the commercial PVDF samples may be assigned to the localized modes associated with the head-to-head or tail-to-tail linkages involved in the samples.

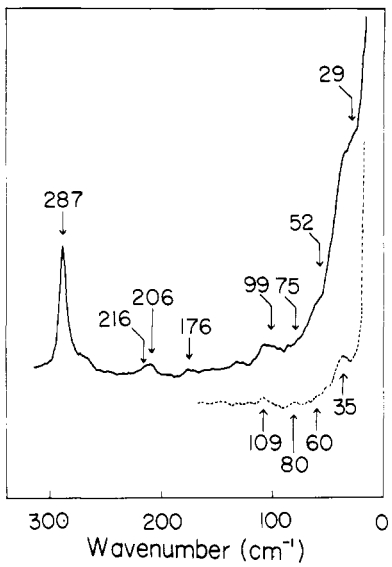

Figure 16 Low-frequency Raman spectra of crystal form II of poly(vinylidene fluoride) measured at room (——) and liquid-nitrogen (- - -) temperature.

Structure and Vibrations of Crystal Form II

If the space group of form II is $P2_1/c$-C_{2s}^5 with two antiparallel chains in the unit cell as proposed by the authors,[2] the number of the optically active normal modes and the selection rules are deduced as given in Table IX. We can expect one librational lattice mode (A_u species) as a perpendicular band in the infrared spectrum and three translational ($2A_g + B_g$) and one librational (B_g) lattice modes in the Raman spectrum. Because two chains in the unit cell correlate with each other by the operation of the center of symmetry, the rule of mutual exclusion should be realized for the lattice modes. The result of the normal coordinate treatment of form II is summarized in Table X.

In the infrared spectrum a sharp perpendicular band appears at 53 cm^{-1}, which shifts to 60 cm^{-1} at liquid-nitrogen temperature. Quite recently Rabolt and Johnson[19] have found independently the same absorption band. This band is assigned to the A_u librational mode, the corresponding calculated frequency being 51 cm^{-1}. In the Raman spectrum we have observed three distinct Raman lines in the low-frequency region, at 99, 52, and 29 cm^{-1} (Figure 16). They are assigned to the translational lattice modes along the *b*, *a*, and *c* axis, respectively. The remaining librational mode with the calculated frequency of 62 cm^{-1} has not yet been observed in the Raman spectrum. The lattice modes are described with the L_x vectors as shown in Figure 17. By the observed frequency data alone, however, we cannot prove the rule of mutual exclusion for the lattice modes.

For the intramolecular vibrations each molecular mode, belonging to the A′ or A″ species of the site symmetry of C_s, splits into two modes in the crystal, one being infrared active and the other Raman active. The frequency gaps due to the intermolecular interactions, as expected from the results of the calculation, may be too small to be detectable by comparing infrared and Raman spectra. In fact they are within experimental errors in frequency measurement as shown in Figure 4. The observed infrared and Raman frequencies of the molecular modes are consistent fairly well with the results of the present calculation based upon the centrosymmetric $P2_1/c$ crystal structure.

Moreover, we cannot find a detectable amount of band splitting in the infrared and Raman spectra measured at liquid-nitrogen temperature, which is, in principle, expected if the crystal lattice belongs to the space group $P2_1$ or

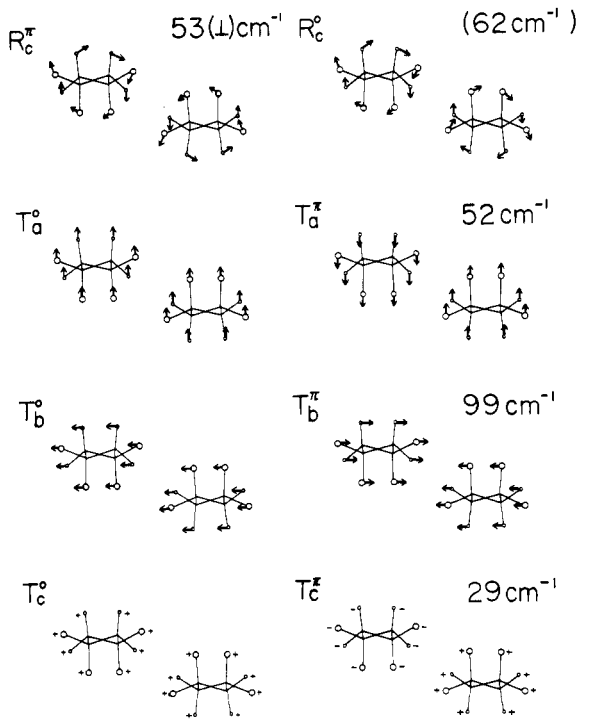

Figure 17. Schematical representation of lattice modes of crystal form II of poly(vinylidene fluoride) with the observed or calculated (in parentheses) frequencies.

$P1$ proposed by Doll and Lando.

Farmer, *et al.*,[8] ascribed the difference in the structures proposed by Doll and Lando and by the authors to the amount of head-to-head defects incorporated in the polymer chains. But the samples of Kynar 201 (amount of head-to-head defects *ca.* 11%) and KF 1000 (supplied by Kureha Chemical Industry Co., Ltd., *ca.* 6%) gave quite the same infrared spectra in our study.

Thus we have no spectroscopic informations which are in conflict with the $P2_1/c$ space group of form II and, therefore, speculate the presence of centrosymmetric lattice, at least as one of the local structures of form II. This does not mean, however, the unique adequacy of the space group. As a general feature of the vibrational spectra of polymeric substances, the observed bands are broad and show rather poor polarization compared with the case of single crystals of nonpolymeric substances. A lot of additional spectral bands, which may be due to the head-to-head linkages or to the noncrystalline region, bring further ambiguities. It is therefore very difficult to deduce a unique conclusion about the packing structures of the polymer crystals from the spectral data alone.

References and Notes

(1) R. Hasegawa, M. Kobayashi, and H. Tadokoro, *Polym. J.*, **3**, 591 (1972).
(2) R. Hasegawa, Y. Takahashi, Y. Chatani, and H. Tadokoro, *Polym. J.*, **3**, 600 (1972).
(3) J. B. Lando, H. G. Olf, and A. Peterlin, *J. Polym. Sci., Part A-1*, **4**, 941 (1966).
(4) G. Natta, G. Allegra, I. W. Bassi, D. Sianesi, G. Caporiccio, and E. Torti, *J. Polym. Sci., Part A*, **3**, 4263 (1965).
(5) G. Cortili and G. Zerbi, *Spectrochim. Acta, Part A*, **23**, 285, 2216 (1967).
(6) W. W. Doll and J. B. Lando, *J. Macromol. Sci., Phys.*, **4**, 897 (1970).
(7) W. W. Doll and J. B. Lando, *J. Macromol. Sci., Phys.*, **4**, 309 (1970).
(8) B. L. Farmer, A. J. Hopfinger, and J. B. Lando, *J. Appl. Phys.*, **43**, 4293 (1972).
(9) S. Enomoto, Y. Kawai, and M. Sugita, *J. Polym. Sci., Part A-2*, **6**, 861 (1968).
(10) F. J. Boerio and J. L. Koenig, *J. Polym. Sci., Part A-2*, **7**, 1489 (1969); **9**, 1517 (1971).

(11) T. Kawauchi and Y. Ishida, private communication.
(12) R. E. Naylor and S. W. Lasoski, *J. Polym. Sci.*, **44**, 1 (1960).
(13) C. W. Wilson and E. R. Santee, *J. Polym. Sci., Part A*, **1**, 1305 (1963).
(14) F. C. Wilson and H. W. Starkweather, Jr., *J. Polym. Sci., Polym. Phys. Ed.*, **11**, 919 (1973).
(15) M. Modena, C. Garbuglio, and M. Ragazzini, *J. Polym. Sci., Part B*, **10**, 153 (1972).
(16) W. W. Doll and J. B. Lando, *J. Macromol. Sci., Phys.*, **2**, 205 (1968).
(17) G. Zerbi, *Pure Appl. Chem.*, **26**, 499 (1971).
(18) R. C. Newman, "Infra-red Studies of Crystal Defects," Taylor and Francis, London, 1973.
(19) J. F. Rabolt and K. W. Johnson, *J. Chem. Phys.*, **59**, 3710 (1973).

Nuclear Magnetic Resonance Relaxation and the Microbrownian Motion in Polymers. Local and Collective Motions and Their Viscosity Dependence

G. Hermann and G. Weill*

Centre de Recherches sur les Macromolécules CNRS, Strasbourg, France.
Received July 19, 1974

ABSTRACT: The loss of orientation memory for a vector linked to a polymer chain is expected to present a fast initial decay corresponding to fast local jumps with a long tail corresponding to diffusive cooperative motions. An analysis of the nuclear relaxation times T_1 and T_2 in solvents of high viscosity where the extreme narrowing condition is not fulfilled may help to separate fast and slow processes. Such an analysis is carried out for poly(oxymethylene) in hexafluoro-2-propanol. The results seem to indicate that both slow and fast processes are linearly dependent on the viscosity, a result of importance for the concept of internal viscosity.

The low-frequency, long-wavelength modes of a polymer chain are adequately described by models derived from the Gaussian subchain model of Rouse.[1] Since in these models the exchange between different subchain conformations corresponding to a given end-to-end vector is supposed to be infinitely rapid, they completely neglect the high-frequency part of the spectrum. Dissipative processes related to the motion inside of a subchain can, however, be taken into account by the introduction of a phenomenological "internal viscosity" parameter.[2] New approaches in the description of polymer dynamics, starting from elementary local motions, have followed the initial work of Verdier and Stockmayer on a cubic lattice.[3-5] They all give the Rouse spectrum in the low-frequency limit, a consequence of the diffusive nature of the fluctuations,[6] but the high-frequency part is very dependent upon the special features of the model. The viscosity dependence of the probability of an elementary jump is of particular interest[7] in connection with the corresponding dependence of the internal viscosity.

Experimental techniques specially adapted to the study of fast movements, such as the dielectric dispersion of chains with a transverse component of the electric moment,[8] fluorescence polarization,[9] line-shape analysis of the paramagnetic resonance of spin labels,[10] and nuclear magnetic resonance,[11] have been used with polymer chains. The response of the chain, in the time or frequency domain, is in all cases related to one autocorrelation function for the rotatory motion of a well defined local molecular unit. But in most cases experiments cover only a limited range of time and frequency and the results can be interpreted assuming a single exponential decay of the autocorrelation function, all fast movements compared to the range of time under study being represented by an instantaneous decay of the autocorrelation function from 1 to a smaller value. This is particularly evident for the polarization of fluorescence where it comes to assume a smaller fundamental polarization. But then the variation of the calculated correlation time with temperature and viscosity will incorporate the approximations made in the choice of the autocorrelation function.[12]

For a model chain in which elementary jumps are supposed to be the exchange of orientation of bonds $i - 1$ and $i + 1$ on a tetrahedral lattice, the complete autocorrelation function has been calculated[13] and found identical with that calculated by Hunt and Powles[14] for the one-dimensional diffusion of a defect, with a fast initial decay and a long $t^{-1/2}$ tail. One can expect this to be a quite general behavior in polymer chains, most of the orientation memory being lost in the first local motions, while a complete loss requires long cooperative motions of the chain. These are required since energetically highly unfavorable conformations, like g^+g^-, generally limit the diffusion by the three bonds mechanism. The relative independence of fast and slow processes finds supports in the calculations of Helfand,[15] who consider the motion of a few segments with Rouse chains at the extremities.

As part of an effort to characterize from an experimental point of view these slow and fast processes we present in this work an nmr relaxation study on simple polymers in solution, where special attention has been paid to the information which can be derived from differences between T_1 and T_2 that is, when the extreme narrowing limit is not completely reached, from the use of measurements on several nuclei (^1H, ^2H, and ^{13}C), and from the viscosity dependence of the relaxation times.

I. Nmr Relaxation Times and Autocorrelation Functions

In the case under study, the nmr relaxation times are governed by the rotation through the autocorrelation function of the second spherical harmonic $P_2(t) = \langle 3\cos^2\theta(t) - 1\rangle/2$ where $\theta(t)$ is the angle of a vector linked to the polymer segment at time t with its original direction at time 0. This vector will be the vector joining two protons, or one proton to the C atom in the case of the dipolar relaxation of the proton and ^{13}C of a CH_2 group, or the axis of the electric field gradient in the case of the quadrupolar relaxation of D.

The expressions for the spin–lattice T_1 and spin–spin T_2 relaxation times are given in the three cases by[16] (a) dipolar relaxation of two ½ identical spins